

COMPARISON OF STANDARD $k-\epsilon$ AND SST $k-\omega$ TURBULENCE MODEL FOR BREASTSHOT WATERWHEEL SIMULATION

Dendy Adanta^{1*}, I. M. Rizwanul Fattah², Nura Muaz Muhammad³

¹Department of Mechanical Engineering, Faculty of Engineering, Universitas Sriwijaya, Indralaya 30662, South Sumatera, Indonesia

²School of Information, Systems and Modelling, University of Technology Sydney, Ultimo, 2007 NSW, Australia

³Faculty of Engineering, Kano University of Science and Technology, Wudil, Nigeria

ABSTRACT

Currently, Computational Fluid Dynamics (CFD) was utilized to predict the performance, geometry optimization or physical phenomena of a breastshot waterwheel. The CFD method requires the turbulent model to predict the turbulent flow. However, until now there is special attention on the effective turbulent model used in the analysis of breastshot waterwheel. This study is to identify the suitable turbulence model for a breastshot waterwheel. The two turbulence models investigated are: standard $k-\epsilon$ model and shear stress transport (SST) $k-\omega$. Pressure based and one degrees of freedom (one-DoF) feature was used in this case with 75 Nm, 150 Nm, 225 Nm and 300 Nm as preloads. Based on the results, the standard $k-\epsilon$ model gave similar result with the SST $k-\omega$ model. Therefore, the simulation for breastshot waterwheel will be efficient if using the standard $k-\epsilon$ model because it requires lower computational power than the SST $k-\omega$ model. However, to study about physical phenomenon, the SST $k-\omega$ model is recommend.

Keywords: Picohydro, Breastshot, Waterwheel, Computational, Turbulent model

1 INTRODUCTION

Indonesia has an abundant energy potential resources that can be converted into electricity by pico hydro turbines [1]. Pico hydro turbines (<5 kW) is one of the suitable types of power plants that can be applied in remote areas [2], since it has the cheapest operational cost and investment when compared with solar PV or wind turbine [3][4]. The pico hydro type breastshot waterwheel is the hydraulic turbine which work effectively in low head condition [2][5]. Moreover, the breastshot waterwheel is environmental friendly due to its harmless nature to aquatic biota [6].

Since the use of breastshot waterwheel is for remote areas, several studies have been carried out to improve its performance. Gotoh, et. al. (2000) [7] examines the different hydraulics behaviours of breastshot with undershot waterwheel. Muller and Wolter (2004) [6] found that the geometry ratio of in- and outflow influenced the performance of a breastshot waterwheel. Quaranta

and Revelli (2015) [8][9] concluded that the factors that affect the performance of a breastshot turbine (losses) is the inflow configurations. Furthermore, Quaranta and Revelli [10][11] improve the inflow configuration by optimizing the shape of the breastshot waterwheel, where they obtained the optimum number of blade configuration. Warjito, et. al. [12] and Budiarmo et al. [13] concluded that the number of blades and kinetic energy of water (EK) influences the performance of the breastshot turbine.

There is an increasing trend of utilization of Computational Fluid Dynamics (CFD) method to predict the performance of breastshot waterwheel. For the CFD method to produce accurate predictions, choice of effective and reliable turbulent approach is necessary. Turbulent flow is characterized by unsteady and irregular movement where its transported variables such as mass, momentum and scalar species fluctuate in space and time. The commonly used computational approaches in turbulent simulation

includes Reynolds Average Navier-Stokes (RANS), Large Eddy simulation (LES) and Direct Numerical Simulation (DNS) [18]. The Reynolds Average Navier-Stokes (RANS) is the commonly used among these turbulent flow approaches. There are many turbulent models based on RANS, where the models are specific to certain flow cases. So, to get accurate results, the turbulent model should be selected. The turbulent $k-\varepsilon$ standard and shear stress transport (SST) $k-\omega$ are models that are widely used both in industrial and academic numerical applications [3].

Although study about breastshot waterwheel has long been done, however until now there has been no specific study about the effect of the use of the turbulent model on its predictions. Therefore, this study will compare the turbulent models $k-\varepsilon$ standard and SST $k-\omega$ in a breastshot waterwheel to identify whether there are significant differences in computational results.

2 METHODOLOGY

2.1 Geometry

This study is a follow-up study by Budiarmo (2018) [13], the geometry used same as the Budiarmo (2018) [13]. The parameters of geometry are listed in Table 1.

Table 1 Parameters of breastshot waterwheel geometry

Parameter	Value
Discharge(Q)	0.05 m ³
Head (H)	1 m
Outer Radius (R_o)	1.04 m
Inner Radius (R_i)	0.67 m
Bucket depth (d)	0.37 m
Filling ratio (ε)	0.5
Lower Section Radius (R_A)	0.37 m
Wheel width (B)	0.25 m
Straight stick length (l)	0.26 m
Stick angle (β)	120°
Water entry angle (α)	26°
Relative entry angle (γ)	50.9°

The schematic parameter in Table 1 can be seen in Figure 1.

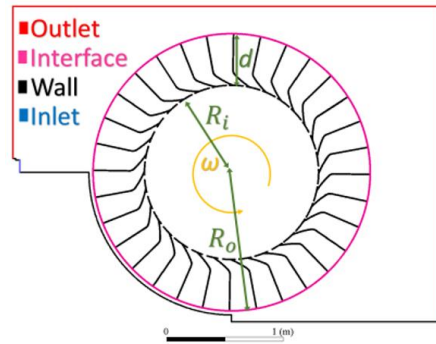


Figure 1 Boundary conditions and geometric dimension

2.2 Turbulence Models

The turbulent flow approach is predicted by using and constructing mathematical model called turbulence model [14][15]. There is no accurate turbulence model for all cases. Understanding the capabilities and limitations of the turbulent models are needed to get the best choice of turbulence model for breastshot waterwheel application.

RANS family models are the models that attempt to approach the turbulence equations using viscosity terms [16]. The kinetic energy turbulent (k) is the base variable calculated. These equations shows the transport equation for mean flow quantities only, with all turbulence scales modeled [16].

2.2.1 Standard $k-\varepsilon$ Turbulence Model

The standard $k-\varepsilon$ model in FLUENT has become the basic model of practical engineering flow calculations since it was proposed by Launder and Spalding [17]. It is a semi-empirical model, and the derivation of this model equations based on phenomenological considerations and empiricism. The standard $k-\varepsilon$ model is valid only for fully turbulent flows. The rate of dissipation (ε) and the turbulence kinetic energy (k) are based from below transport equations [18]:

$$\frac{\partial}{\partial t}(\rho k) + \frac{\partial}{\partial x_i}(\rho k u_i) = \frac{\partial}{\partial x_j} \left[\left(\mu + \frac{\mu}{\sigma_k} \right) \frac{\partial k}{\partial x_j} \right] + G_k + G_b - \rho \varepsilon - Y_M + S_k \quad (1)$$

and

$$\begin{aligned} \frac{\partial}{\partial t}(\rho\varepsilon) + \frac{\partial}{\partial x_i}(\rho\varepsilon u_i) = \frac{\partial}{\partial x_j} \left[\left(\mu + \frac{\mu}{\sigma_\varepsilon} \right) \frac{\partial \varepsilon}{\partial x_j} \right] + C_{1\varepsilon} \frac{\varepsilon}{k} (G_k + C_{3\varepsilon} G_b) + C_{2\varepsilon} \rho \frac{\varepsilon^2}{k} + S_\varepsilon \end{aligned} \quad (2)$$

where G_k represents the generation of turbulence kinetic energy due to the mean velocity gradients. G_b is the generation of turbulence kinetic energy due to buoyancy, Y_M represents the contribution of the fluctuating dilatation in compressible turbulence to the overall dissipation rate, $C_{1\varepsilon}$, $C_{2\varepsilon}$, and $C_{3\varepsilon}$ are constants. σ_k and σ_ε are the turbulent Prandtl numbers for k and ε , respectively. S_k and S_ε are user-defined source terms.

2.2.2 Shear Stress Transport (SST) k- ω Turbulence Model

The SST k- ω model are model effectively for prediction flow in the near-wall region [19]. The SST k- ω model is similar to the standard k- ω model, but the turbulent viscosity is modified where in SST k- ω rotating tensor and blending function are included [19], [20]. The SST k- ω model has a blending function and the addition of a cross-diffusion term in the ω equation and to ensure that the model equations behave appropriately in both far-field zones and the near-wall [19], [20]. The specific dissipation rate (ω) and the turbulence kinetic energy (k) are obtained from the following transport equations [14]:

For k :

$$\begin{aligned} \frac{\partial}{\partial t}(\rho k) + \frac{\partial}{\partial x_i}(\rho k u_i) = \frac{\partial}{\partial x_j} \left[\Gamma_k \frac{\partial k}{\partial x_j} \right] + G_k - Y_k + S_k \end{aligned} \quad (3)$$

And for ω :

$$\begin{aligned} \frac{\partial}{\partial t}(\rho\omega) + \frac{\partial}{\partial x_i}(\rho\omega u_i) = \frac{\partial}{\partial x_j} \left[\Gamma_\omega \frac{\partial \omega}{\partial x_j} \right] + G_\omega - Y_\omega + D_\omega + S_\omega \end{aligned} \quad (4)$$

where G_ω represents the generation of ω , G_k represents the generation of k due to mean velocity gradients, Γ_k and Γ_ω represent the effective diffusivity of k and ω , respectively. Y_ω and Y_k represent the dissipation of ω and k in the turbulence, D_ω represents the cross-diffusion term. S_ω and S_k are user-defined source terms.

2.3 Simulation Setup

This CFD simulation was performed by using the ANSYSTM Fluent 18.2 Academic Version. The simulation was done at 0.002 s / time step and 4000 timesteps, this simulation runs for 8 seconds. Water and air are used as working fluids. The water is determined as the main phase with a constant surface pressure to the second phase (air) at 0.0728 N/m. The multiphase approach of volume of fluid (VoF) was used with the implicit volume of the model fluid used as an implicit body force. Pressure base was imposed at the Inlet and outlet boundaries with total pressure being 490.5 Pa and 0 Pa at the inlet and outlet respectively. The backflow setting of the air phase must be set to 1 to ensure there is no water allowed in except from the inlet. The initial value in inlet is 1 (there is no air in inlet). The prediction of wheel rotation was done using one degree of freedom (one-DoF). The one-DoF feature with moment of inertia set to 125 kg.m². The one-DoF requires preload, the preload used is: 75N·m, 150 N·m, 225 N·m, and 300 N·m.

2.4 Simulation Independency Test

Before the simulation data is processed, an independence test was performed to obtain the optimum mesh size and timestep. The grid/mesh independency tests done using k- ε standard turbulence model. The mesh independence test is done with three number of meshes: 30000 of mesh normalized elements (NGS) to 4; 123000 to 2; and 493000 to 1. In mesh independency test, the wheel condition is static. Richardson extrapolation method is used to determine the error each number of mesh or called grid convergency index (GCI). In general, the greater number of the mesh element, will produced the smaller error. The acceptable error from GCI analysis is below 3%. After the mesh independency test, next step is timestep independency test. Since there is no standard method for determining timestep size so, for this case, timestep independency using concept GCI called timestep convergency index (TCI). There are three timestep size: 0.002 s normalized timestep spacing (NTS) to 1; 0.004 s to 2; and 0.008 s to 4.

3 RESULTS AND DISCUSSIONS

3.1 Independency Test Results

Torque is used to mesh and timestep independency test. The results of mesh and timestep independency test is briefly displayed in

Table 2 and Table 3, respectively. From Table 2, the timestep size of 0.002 s used because it has an error below 2%. While, from Table 3, number of mesh of 123,000 elements used because it has an error of below 1%.

Table 2 Timestep independency test result

NTS	Time size	Torque (Nm)	GCI (%)
0	Continuum	202.12	0
1	0.002 s	197.19	1.78
2	0.004 s	190.25	2.59
4	0.008 s	173.55	6.84

Table 3 Mesh independency test result

NTS	Elements	Torque (Nm)	GCI (%)
0	<i>infinity</i>	404.47	0
1	493000	405.17	0.01
2	123000	413.86	0.17
4	30000	529.97	2.27

3.2 Waterwheel's Simulation Result

The results of the simulation are obtained for the eddy viscosity contours, turbulent intensity, and torque. From Figure 2, there is significant difference in the viscosity eddy contour between the standard k- ϵ model with the SST k- ω . The standard k- ϵ model shows more eddy viscosity activity on the turbine blade than the SST k- ω model due to adverse pressure gradient that disturbed the boundary layer. Since the SST k- ω model has damps coefficient for turbulent viscosity causing a low-Reynolds-number correction (α^*), thus, the visible turbulence is not as much as in the standard k- ϵ turbulent model or k- ϵ near wall scalable.

In Figure 3, for turbulent intensity, there is no significant difference in the viscosity eddy contour between the standard k- ϵ with the SST k- ω model. This is allegedly in the near wall, effective viscosity calculation by the effect of near wall is not significant in the standard k- ϵ with the SST k- ω model similar results. In addition, a modified turbulent viscosity equation (3) introduced to cater for transport effects of the major turbulent shear stress helped in the intensification of turbulence.

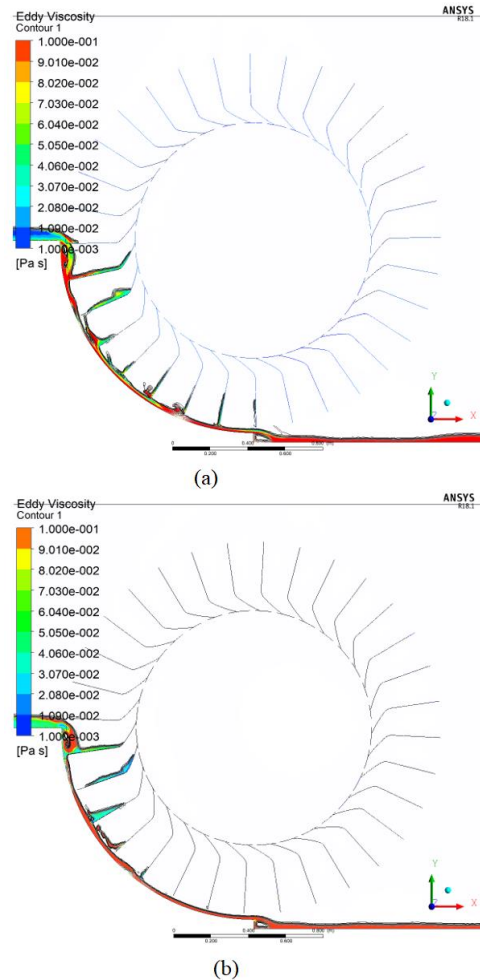


Figure 2 Eddy viscosity contour of 150 Nm preload for: (a) Standard k- ϵ and (b) SST k- ω

In Figure 4, for the torque, there is no significant difference of prediction of torque. The prediction torque by standard k- ϵ model and the SST k- ω model show almost the same graphical pattern. So, for the simulation test using Torque as variable, it's more preferable to use the standard k- ϵ because it has lower computational time than the SST k- ω model.

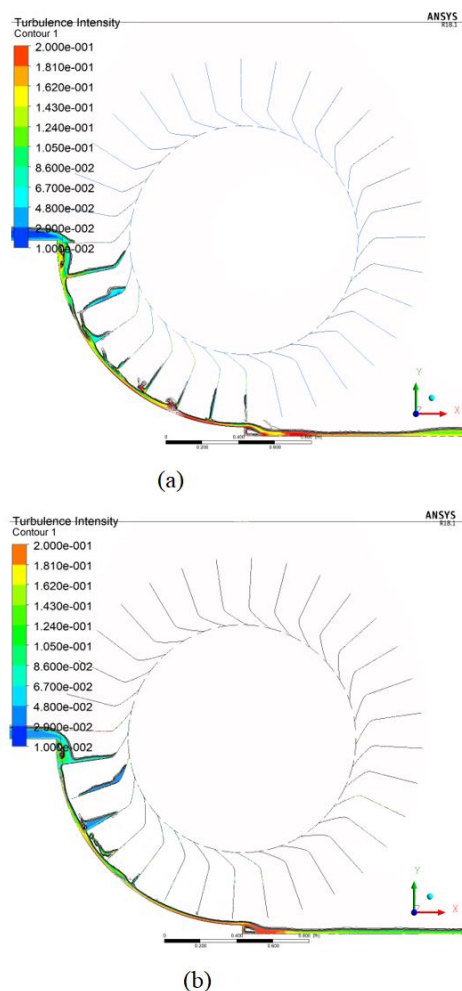


Figure 3 Turbulence intensity contour of 150 Nm preload for: (a) Standard $k-\epsilon$ and (b) SST $k-\omega$

4 CONCLUSIONS

The standard $k-\epsilon$ model and the SST $k-\omega$ model gives the close result for simulation of breastshot waterwheel, so for more efficient and reliable result, it's better to use the standard $k-\epsilon$ model because it has lower computing power than the SST $k-\omega$ model. However, to study about physical phenomenon in breastshot waterwheel such as the eddy viscosity and the turbulence intensity, the SST $k-\omega$ model is recommend.

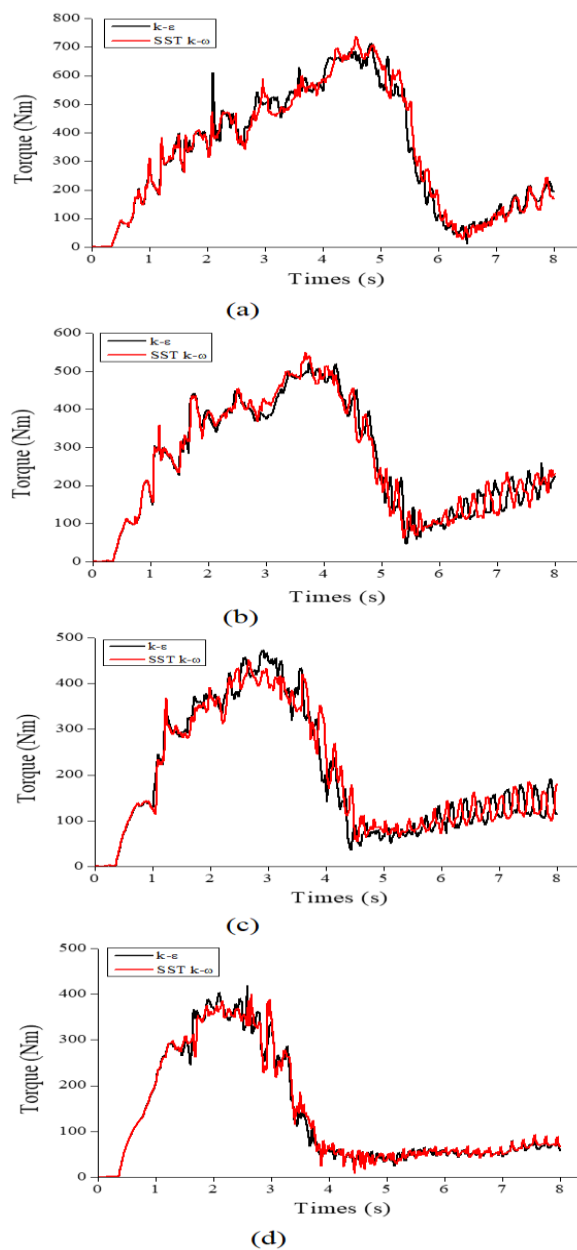


Figure 4 Torque residuals for different Preloads of: (a) 300Nm, (b) 225 Nm, (c) 150 Nm and (d) 75 Nm

REFERENCES

- [1] Warjito, D. Adanta, Budiarmo, and A. P. Prakoso, "The Effect of Bucket Number on Breastshot Waterwheel Performance," in *IOP Conference Series: Earth and Environmental Science*, 2018, p. 12031.
- [2] B. Ho-Yan, "Design of a Low Head Pico Hydro Turbine for Rural Electrification in Cameroon," University of Guelph, 2012.
- [3] D. Adanta, Budiarmo, Warjito, and A. I. Siswantara, "Assessment of Turbulence Modelling for Numerical Simulations into Pico Hydro Turbine," *Journal of Advanced Research in Fluid Mechanics and Thermal Sciences*, vol. 45, pp. 21–31, 2018.
- [4] P. Adhikari, U. Budhathoki, S. R. Timilsina, S. Manandhar, and T. R. Bajracharya, "A Study on Developing Pico Propeller Turbine for Low Head Micro Hydropower Plants in Nepal," *Journal of the Institute of Engineering*, vol. 9, no. 1, pp. 36–53, 2014.
- [5] S. J. Williamson, B. H. Stark, and J. D. Booker, "Low Head Pico Hydro Turbine Selection Using a Multi-Criteria Analysis," *Renewable Energy*, vol. 61, pp. 43–50, 2014, doi: 10.1016/j.renene.2012.06.020.
- [6] G. Muller and C. Wolter, "The Breastshot Waterwheel: Design and Model Tests," *ICE Proceedings-Engineering Sustainability*, pp. 203–211, 2004.
- [7] M. Gotoh, H. Kowata, T. Okuyama, and S. Katayama, "Damming-up Effect of a Current Water Wheel Set in a Rectangular Channel," *World Renewable Energy Congress VI*, pp. 1615–1618, Jan. 2000, doi: 10.1016/B978-008043865-8/50333-0.
- [8] E. Quaranta and R. Revelli, "Optimization of Breastshot Water Wheels Performance Using Different Inflow Configurations," *Renewable Energy*, vol. 97, pp. 243–251, 2016, doi: 10.1016/j.renene.2016.05.078.
- [9] E. Quaranta and R. Revelli, "Performance Characteristics, Power Losses and Mechanical Power Estimation for a Breastshot Water Wheel," *Energy*, vol. 87, pp. 315–325, 2015, doi: <http://dx.doi.org/10.1016/j.energy.2015.04.079>.
- [10] E. Quaranta and R. Revelli, "CFD Simulations to Optimize the Blades Design of Water Wheels," *Drinking Water Engineering and Science Discussions*, pp. 1–8, Jan. 2017, doi: 10.5194/dwes-2017-2.
- [11] E. Quaranta and R. Revelli, "Hydraulic Behavior and Performance of Breastshot Water Wheels for Different Numbers of Blades," *Journal of Hydraulic Engineering*, vol. 143, no. 1, p. 4016072, 2016.
- [12] Warjito, D. Adanta, Budiarmo, and A. P. Prakoso, "The Effect of Bucketnumber on Breastshot Waterwheel Performance," in *IOP Conference Series: Earth and Environmental Science*, 2018, vol. 105, no. 1, p. 12031.
- [13] Budiarmo, Warjito, J. S. PPS, A. P. Prakoso, and D. Adanta, "Influence of Bucket Shape and Kinetic Energy on Breastshot Waterwheel Performance," in *2018 4th International Conference on Science and Technology (ICST)*, 2018, pp. 1–6.
- [14] T. Saad, "Turbulence Modeling for Beginners," *University of Tennessee space institute*, 2011.
- [15] H. Tennekes and J. L. Lumley, *A first course in turbulence*. MIT press, 1972.
- [16] L. Davidson, *Fluid mechanics, turbulent flow and turbulence modeling*. Chalmers University of Technology, 2015.
- [17] B. E. Launder and D. B. Spalding, "The Numerical Computation of Turbulent Flows," *Computer Methods in Applied Mechanics and Engineering*, vol. 3, no. 2, pp. 269–289, 1974, doi: 10.1016/0045-7825(74)90029-2.
- [18] ANSYS, "Turbulence," in *ANSYS FLUENT 12.0 Theory Guide*, 2009, pp. 2-1-4–46.
- [19] F. R. Menter, "Two-Equation Eddy-Viscosity Turbulence Models for Engineering Applications," *AIAA journal*, vol. 32, no. 8, pp. 1598–1605, 1994.
- [20] F. R. Menter, "Improved Two-Equation k-Omega Turbulence Models for Aerodynamic Flows," 1992.